ChemPubSoc Europe

DOI: 10.1002/chem.201802188

CHEMISTRY
A European Journal
Full Paper

Cage Compounds |Hot Paper|

Donor-Site-Directed Rational Assembly of Heteroleptic *cis*-[$Pd_2L_2L'_2$] Coordination Cages from Picolyl Ligands

Rongmei Zhu+,[a, b] Witold M. Bloch+,[a, c] Julian J. Holstein,[a] Soham Mandal,[a] Lars V. Schäfer,[d] and Guido H. Clever*[a]

Abstract: A donor-site engineering approach facilitates the formation of heteroleptic [$Pd_2\mathbf{L}_2\mathbf{L}'_2$]$^{4+}$ cage structures through a favored *cis*-'in$_2$/out$_2$' spatial configuration of the methyl groups of 5- and 3-substituted bis-monodentate picolyl ligands with flat acridone and bent phenothiazine backbones. The heteroleptic cages were confirmed by ESI-MS and 2D NMR experiments as well as DFT calculations, which pointed toward a *cis*-configuration being energetically favored. This was further supported by the synthesis and X-ray structure of a previously unreported *cis*-[Pd(2-picoline)$_4$]$^{2+}$ complex. The formation of homoleptic structures, however, was met with considerable steric hindrance at the Pd^{II} centers, as observed by the formation of [$Pd_2\mathbf{L}_3$(solvent)$_2$]$^{4+}$ and [$Pd_2\mathbf{L}_2$(solvent)$_4$]$^{4+}$ species when only one type of acridone-based ligand was offered. In contrast, bent phenothiazine ligands with outside-pointing methyl groups showed the ability to form interpenetrated double-cages, as revealed by X-ray crystallography. The general route presented herein enables the assembly of uniform *cis*-[$Pd_2\mathbf{L}_2\mathbf{L}'_2$]$^{4+}$ coordination cages, thus furthering the possibility to increase structural and functional complexity in supramolecular systems.

Introduction

Nature provides elegant pathways for the assembly of complex and functional multi-component systems by combining strong chemical bonds with weak supramolecular interactions in a controlled and harmonious manner. These principles form the basis of a toolbox for chemists who seek to increase the molecular complexity of artificial nanoscopic systems. In the field of metallosupramolecular chemistry, significant efforts have been directed toward controlling the assembly of discrete, heteroleptic structures formed by metal–ligand bonding.[1] In this context, methods involving steric control have been particularly successful in regulating multiple different ligands around a single metal center. Early on, Lehn reported the assembly of multi-component heteroleptic architectures by exploiting steric constraints in combination with principles of maximum site occupancy.[2] Among several approaches building on from this, Schmittel's HETPHEN[3] methodology (and related variations) has been extensively utilized to assemble a wide variety of 2D and 3D prismatic heteroleptic assemblies.[1a,4] Similar structures have also been assembled through a related approach developed by Fujita and Yoshizawa, termed "side-chain-directed" assembly, which features sterically controlled heteroleptic coordination of lutidine and pyridine donors to *cis*-chelated square-planar metal centers (Figure 1 a).[5] Whilst the latter strategy provides reliable routes to heteroleptic structures composed of *cis*-chelated metal centers with two pendant binding sites, strategies to control the heteroleptic coordination environment of "naked" square-planar metal centers and multiple bis-monodentate ligands in metallosupramolecular assemblies are still in early development.[6]

[M_2L_4] coordination cages assembled from square-planar metal cations (M = Pd^{II}, Pt^{II}, Cu^{II}, Ni^{II}) and bis-monodentate banana-shaped ligands are a diverse class of hosts that possess a well-ordered central cavity.[7] By incorporating chosen functionalities into the ligand components, a variety of homoleptic [$Pd_2\mathbf{L}_4$] cages have been prepared, exhibiting functions such as

[a] *Dr. R. Zhu,+ Dr. W. M. Bloch,+ Dr. J. J. Holstein, Dr. S. Mandal, Prof. Dr. G. H. Clever*
Faculty of Chemistry and Chemical Biology
TU Dortmund University
Otto-Hahn-Strasse 6, 44227 Dortmund (Germany)
E-mail: guido.clever@tu-dortmund.de

[b] *Dr. R. Zhu+*
Current affiliation: School of Chemistry and Chemical Engineering
Yangzhou University
225002 Yangzhou, Jiangsu (P.R. China)

[c] *Dr. W. M. Bloch+*
Current affiliation: Department of Chemistry and Centre for Advanced Nanomaterials
School of Physical Sciences
The University of Adelaide, Adelaide (Australia)

[d] *Prof. Dr. L. V. Schäfer*
Center for Theoretical Chemistry
Faculty of Chemistry and Biochemistry
Ruhr-University, 44780 Bochum (Germany)

[+] *These authors contributed equally to this work.*

Supporting information and the ORCID identification number(s) for the author(s) of this article can be found under: https://doi.org/10.1002/chem.201802188.

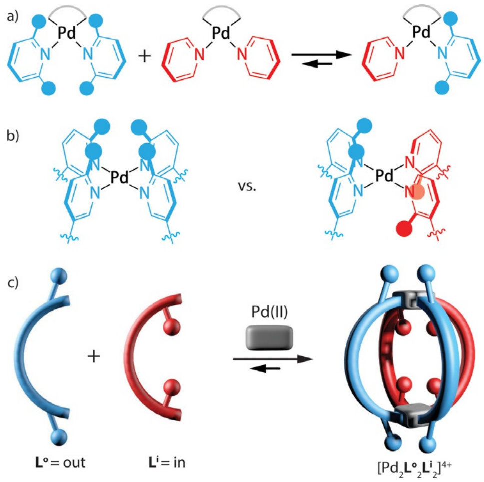

Figure 1. a) Yoshizawa and Fujita's side chain-directed approach of *cis*-chelated Pd^{II} nodes; b) this work's picoline *cis*-'in$_2$/out$_2$' approach in which the *meta*-relationship of the coordinating nitrogen and the backbone attachment forbids rotation of the donor; c) schematic representation of the assembly of a heteroleptic *cis*-[Pd$_2$**L°**$_2$**L^i**$_2$] cage from picoline-derived ligands with outside (**L°**) and inside (**L^i**) pointing methyl groups.

light switchability,[8] redox activity,[9] neutral[10] and charged guest encapsulation,[11] drug delivery,[12] endohedral rotary dynamics[13] and structural transformations.[14] So far, the majority of such cages have been equipped with only a single function each, owing to the limitations in controlling the coordination of different ligands around the same square-planar metal center. It is envisioned that grafting more than one of these functionalities into an assembly will provide new multifunctional host structures. Entropy, however, usually thwarts this objective, due to the tendency of mixed-ligand metal-mediated reactions to form statistical or, alternatively, narcissistically self-sorted mixtures.[15] Driving the system toward integrative self-sorting, where only one defined heteroleptic product is formed from a mix of ligands, can therefore be a challenging task. Nevertheless, approaches to control the arrangement and assembly of template-free [M$_2$**L**$_2$**L′**$_2$] cages are currently being developed in several groups.[6b, 15b, 16] For example, Crowley reported a strategy to achieve kinetically trapped *cis*-[Pd$_2$**L**$_2$**L′**$_2$] cages through ligand substitution reactions of an unfunctionalized homoleptic cage precursor with 2-amino-functionalized pyridyl ligands.[16b] Recently, we reported that [Pd$_2$**L**$_2$**L′**$_2$] cages can be accessed by utilizing ligands of complementary shape. This strategy facilitated the assembly of a template-free *cis*-heteroleptic cage under thermodynamic control, which was utilized for the shape-discrimination of guest stereoisomers.[17] We further showed that geometric constraints can lead to the integrative self-sorting of a unique *trans*-[Pd$_2$(*anti*-**L**)$_2$**L′**$_2$] self-penetrating cage with inherent structural chirality.[18]

Herein we present a new approach to reliably generate regular-shaped *cis*-[Pd$_2$**L**$_2$**L′**$_2$] cages through steric control of the spatial configuration of picolyl (pic) ligands around the Pd^{II} center (Figure 1 b). As a key design feature, the picoline donors are connected to the backbone via their *meta* positions, thus fixing the methyl substituent in either an "inside" (*ortho* to the backbone connection) or "outside" (*para* to the backbone connection) orientation with respect to the cage's cavity. We further show that two different backbones, acridone and phenothiazine, can be successfully combined in one assembly. Consequently, this approach enables two electronically distinct moieties to be configurationally fastened in a regular-shaped cage assembly.

Results and Discussion

Ligand synthesis and homoleptic cage assembly

The picolyl ligands **A°**, **A′°**, **A^i**, **P°** and **P^i** (**A** = acridone, **P** = phenothiazine, **o** = picoline out, **i** = picoline in, Scheme 1) were synthesized via Sonogashira cross-coupling reactions between 5- or 3-ethynyl-2-picoline and the respective dibromo-acridone or phenothiazine backbone precursors. In order to distinguish between homoleptic and heteroleptic assemblies by means of mass spectrometry, we installed exohedral hexyl (**A°**, **A^i** and **P°**) or octyl (**A′°**, **P^i**) substituents into the central part of the respective ligand backbones (Supporting Information).

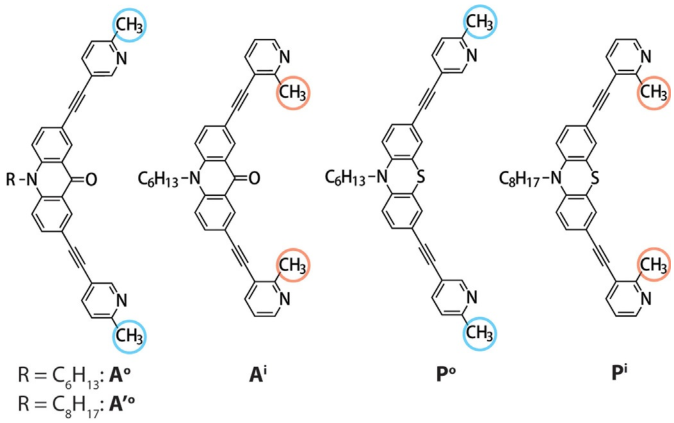

Scheme 1. The acridone and phenothiazine picolyl ligands investigated in this study (all ligands carry hexyl chains, only **A′°** and **P^i** comprise octyl chains).

Before investigating heteroleptic structures, we first examined homoleptic self-assembly of the picolyl functionalized ligands. We postulated that the apparent steric hindrance encountered in homoleptic Pd^{II} assemblies (possessing only one type of the above-mentioned ligands) may hinder homoleptic [Pd$_2$**L**$_4$] cage formation.

Initially, heating a 2:1 mixture of **A^i** and [Pd(CH$_3$CN)$_4$](BF$_4$)$_2$ in CD$_3$CN at 70 °C for 8 h gave a convoluted mixture, as revealed by ^{1}H NMR spectroscopy. Performing the reaction at room temperature, however, resulted in a more homogeneous sample that exhibited two sets of proton peaks in a ratio of 2:1 in the ^{1}H NMR spectrum (Figure 2 a,c). Compared to the free ligand, a downfield shift of proton signals H_f and H_g was observed, indicating Pd^{II} complexation. Analysis of the sample by ESI-MS (Figure S20) revealed a prominent peak consistent with the formula [Pd$_2$**A^i**$_3$(CH$_3$CN)$_2$]$^{4+}$, alongside other peaks corresponding to the formula [Pd$_2$**A^i**$_3$(F)$_n$]$^{(4-n)+}$ (n = 1, 2). The presence of

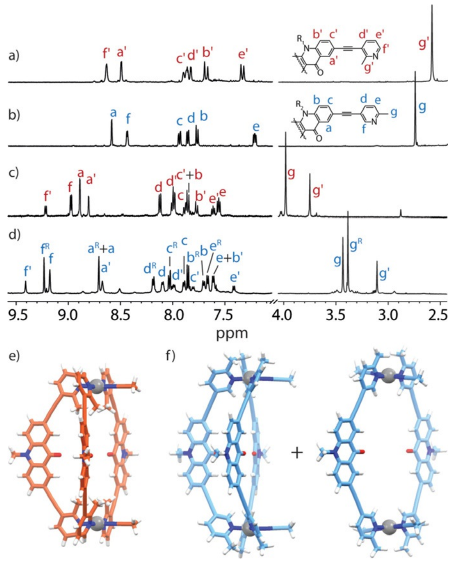

Figure 2. ^{1}H NMR spectra (500 MHz/CD_3CN) of a) $\mathbf{A^i}$; b) $\mathbf{A'^o}$; c) $[Pd_2\mathbf{A^i}_3(CD_3CN)_2]^{4+}$; d) a 1:1 mixture of $[Pd_2\mathbf{A'^o}_3(CD_3CN)_2]^{4+}$ and $[Pd_2\mathbf{A'^o}_2(CD_3CN)_4]^{4+}$; e) DFT calculated structure of bowl compound formed from the reaction of $\mathbf{A^i}$ and Pd^{II}: $[Pd_2\mathbf{A^i}_3(CD_3CN)_2]^{4+}$(Pd⋅⋅⋅Pd distance = 16.0 Å); f) calculated structures of the products formed from the reaction of $\mathbf{A'^o}$ and Pd^{II}: $[Pd_2\mathbf{A'^o}_3(CD_3CN)_2]^{4+}$ and $[Pd_2\mathbf{A'^o}_2(CD_3CN)_4]^{4+}$ (Pd⋅⋅⋅Pd distances = 17.3 and 17.5 Å, respectively).

fluoro ligands is presumably due to contaminations of hydrolyzed tetrafluorborate resulting in F^- anions occupying the free Pd^{II} coordination sites.[19] ^{1}H -^{1}H NOESY analysis (Figure S19) revealed cross peaks between the two observed sets of NMR signals (e.g. H_f⋅⋅⋅$H_{f'}$), indicating their close proximity within the same structure. This was further supported by a DOSY experiment, which revealed that the two sets of proton signals correspond to the same diffusion coefficient (log D = −9.23, Figure S24). The NMR data is consistent with $[Pd_2\mathbf{A^i}_3(CD_3CN)_2]^{4+}$ possessing a bowl-shaped structure with C_{2v} symmetry, with two of the three ligands being chemically equivalent (Figure 2 e). Eventually, evidence for the partial formation of a $[Pd_2\mathbf{A^i}_4]^{4+}$ cage was obtained by ESI-MS analysis after heating the sample at 70 °C for 8 h, although the ^{1}H NMR spectrum revealed the presence of free ligand, suggesting that $[Pd_2\mathbf{A^i}_3(CD_3CN)_2]^{4+}$ decomposes at elevated temperatures (Figures S21–S25).

Combining $\mathbf{A'^o}$ with $[Pd(CH_3CN)_4](BF_4)_2$ in 2:1 ratio at 25 °C produced yet a more complicated ^{1}H NMR spectrum, with three sets of proton peaks in a 2:1:2 ratio (Figure 2 b,d). COSY, NOESY and ESI-MS analysis confirmed that, like for $\mathbf{A^i}$, two sets of proton signals (2:1 ratio) originate from a bowl-shaped $[Pd_2\mathbf{A'^o}_3(CD_3CN)_2]^{4+}$ species (Figures S26–S29). The remaining set of signals was assigned to a ring-like $[Pd_2\mathbf{L}_2(CD_3CN)_4]^{4+}$ structure due to several peaks in the mass spectrum corresponding to a formula $[Pd_2\mathbf{A'^o}_2+n BF_4]^{(4-n)+}$ (n = 1, 2). In this case, heating the sample at 70 °C did not result in conversion to a $[Pd_2\mathbf{L}_4]$ coordination cage, suggesting that the degree of steric crowding above the Pd^{II} planes significantly hinders cage formation.

A comparison of the DFT-optimized homoleptic structures (Figure 2 e,f) revealed notable differences between the picolyl-*in* versus picolyl-*out* $[Pd_2\mathbf{L}_3(CH_3CN)_2]^{4+}$ assemblies. For example, the difference in the Pd⋅⋅⋅Pd distance in the calculated structures of $[Pd_2\mathbf{A^i}_3(CH_3CN)_2]^{4+}$ and $[Pd_2\mathbf{A'^o}_3(CH_3CN)_2]^{4+}$ (16.0 versus 17.3 Å, respectively), shows the contracting or elongating effect that steric crowding has on the overall structure. In particular, the missing fourth ligand seems to allow the bowl-shaped structures to adapt to the steric bulk introduced by the methyl substituents by attaining a more convex or concave shape, respectively.

The co-formation of $[Pd_2\mathbf{A'^o}_2(CH_3CN)_4]^{4+}$ (Figure 2 f) along with $[Pd_2\mathbf{A'^o}_3(CH_3CN)_2]^{4+}$ suggests that ligation of the metal centers is hindered more from the steric crowding of picoline donors on the outside of the Pd^{II} planes, rather than on the inner face of the Pd^{II} planes (with respect to the cage's cavity; however, compare the observation of homoleptic double-cage formation from $\mathbf{P^o}$ as discussed below).

It is worth noting that bowl-shaped $[Pd_2\mathbf{L}_3]^{4+}$ compounds have seldom been reported.[20] Additionally, the isolation of $[Pd_2\mathbf{L}_2(solvent)_2]^{4+}$ macrocycles is rare,[21] as they are more often encountered when the Pd^{II} centers possess additional *cis*-[22] or *trans*-chelating ligands.[23]

Heteroleptic cage assembly from acridone ligands

Given the notable degree of steric hindrance encountered in the homoleptic structures, we hypothesized that a $[Pd_2\mathbf{L}_2\mathbf{L'}_2]^{4+}$ heteroleptic structure, in which the picoline donors are oriented *anti* with respect to one another, may alleviate the degree of steric crowding. Indeed, heating a 1:1:1 mixture of $\mathbf{A'^o}$, $\mathbf{A^i}$ and $[Pd(CH_3CN)_4](BF_4)_2$ for 8 h resulted in a distinct ^{1}H NMR spectrum, relative to the homoleptic assemblies of the two ligands (Figure 3 a). In this case, two sets of signals with equal integral ratios, corresponding to the two ligating components ($\mathbf{A^i}$ and $\mathbf{A'^o}$), were observed. An ESI-MS measurement revealed prominent peaks which could be assigned to $[Pd_2\mathbf{A^i}_2\mathbf{A'^o}_2+n BF_4]^{(4-n)+}$ (n = 0, 1; Figure 3 b and S35), as the hexyl chains of $\mathbf{A^i}$ and octyl chains of $\mathbf{A'^o}$ provided unambiguous *m/z* differentiation from any homoleptic cage analogues. Further evidence for a heteroleptic structure was provided by ^{1}H-^{1}H NOESY analysis, which revealed important cross peaks between the two

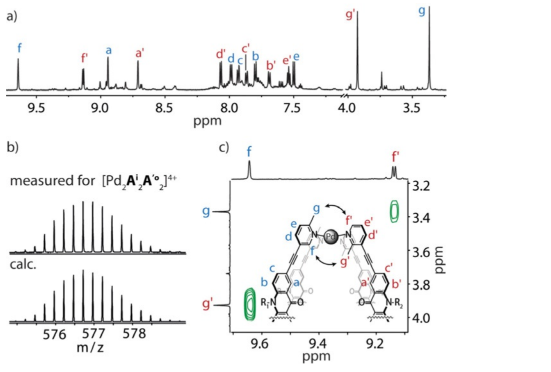

Figure 3. a) ^{1}H NMR spectrum (600 MHz/CD_3CN) of $[Pd_2\mathbf{A^i}_2\mathbf{A'^o}_2]^{4+}$; b) measured and calculated isotope pattern of $[Pd_2\mathbf{A^i}_2\mathbf{A'^o}_2]^{4+}$; c) part of the ^{1}H -^{1}H NOESY spectrum showing the inter-ligand contacts between adjacent picolyl ligands.

adjacent ligands: $H_f\cdots H_{g'}$ and $H_{f'}\cdots H_g$ (Figure 3c, Figure S33). In addition to this, DOSY analysis confirmed that the assigned signals of $[Pd_2\mathbf{A}^i{}_2\mathbf{A'}^o{}_2]^{4+}$ correspond to the same diffusion coefficient (log $D=-9.26$, Figure S34).

Interestingly, we were also able to achieve the same heteroleptic structure through a cage-to-cage rearrangement of the respective homoleptic $[Pd_2\mathbf{L}_3(CH_3CN)_2]^{4+}$ derivatives (Figure S31) indicating that the heteroleptic $[Pd_2\mathbf{A}^i{}_2\mathbf{A'}^o{}_2]^{4+}$ cage is the thermodynamic minimum of the system.

Investigation into cage configuration

Despite numerous attempts, growth of crystals of $[Pd_2\mathbf{A}^i{}_2\mathbf{A'}^o{}_2]^{4+}$, suitable for X-ray structure elucidation, was unfruitful. In order to determine whether the *cis* or *trans* configuration is favored in this system, we performed DFT calculations on the heteroleptic *cis*- and *trans*-$[Pd_2\mathbf{A}^i{}_2\mathbf{A'}^o{}_2]^{4+}$ cages (with truncated side chains) using a number of different functionals and basis sets (Supporting Information). Here, all of the calculations point toward the *cis* structure as the lower energy conformer, however, the energy difference between the two isomers is rather modest, ranging from 4.3 kJ mol^{-1} to 9.3 kJ mol^{-1} in favor of *cis*-$[Pd_2\mathbf{A}^i{}_2\mathbf{A'}^o{}_2]^{4+}$.

To provide further insight into the heteroleptic cage configuration, we investigated the synthesis and structure of a discrete $[Pd(2\text{-pic})_4]^{2+}$ complex, serving as the minimal structural model of the part of the cages that controls the ligand arrangement. Interestingly, a literature search revealed that $[M(2\text{-pic})_4]^{2+}$ structures, in general, have seldom been reported[24] and their preferred conformations are unknown. $[Pd(2\text{-pic})_4](BF_4)_2$ was prepared by heating $[Pd(CH_3CN)_4](BF_4)_2$ in 2-picoline at 70 °C for 0.5 h. Single crystals were obtained directly from the reaction mixture by slow evaporation of the excess 2-picoline. In accordance with the calculated preference for the cage's *cis*-isomer, the X-ray analysis revealed the structure to be *cis*-$[Pd(\textit{up}\text{-2-pic})_2(\textit{down}\text{-2-pic})_2](BF_4)_2$ (descriptors *cis*, *up*, and *down* with respect to the relative position of the methyl substituents), with all four Pd–N bonds in the range of 2.04 ± 0.01 Å. A PXRD measurement of the sample revealed an excellent agreement between the experimental and calculated patterns (Figure 4c), indicating that $[Pd(\textit{up}\text{-2-pic})_2(\textit{down}\text{-2-pic})_2](BF_4)_2$ is also *cis*-configured in the bulk solid. Interestingly, the ^{1}H NMR spectrum of the as-prepared complex dissolved in MeOD revealed twofold signal splitting and broadening at room temperature, indicating two conformations to be in slow exchange (most probably the *cis* and *trans* arrangements) and coalescence to one set of signals above 50 °C. Dissolution of crystals of *cis*-$[Pd(\textit{up}\text{-2-pic})_2(\textit{down}\text{-2-pic})_2](BF_4)_2$ in coordinating solvents such as CD_3CN resulted in slow decomposition of the complex into a convoluted mixture over a period of 1 week (Figure S15), pointing towards a certain lability of the mononuclear complex when dissolved in a competitive solvent. For the cage structures, however, the bridging nature of the bis-monodentate ligands was found to result in a stable structure and no decomposition was observed in solution over extended time periods.

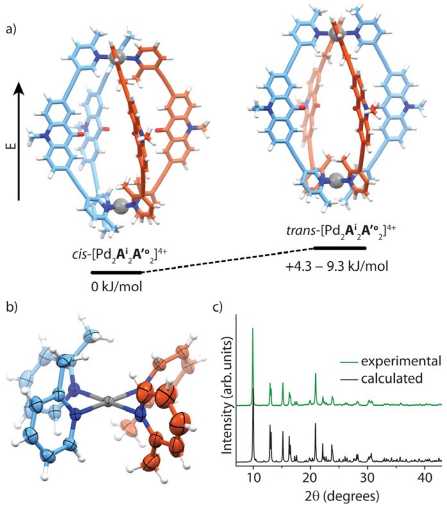

Figure 4. a) Models of *cis*-$[Pd_2\mathbf{A}^i{}_2\mathbf{A'}^o{}_2]^{4+}$ and *trans*-$[Pd_2\mathbf{A}^i{}_2\mathbf{A'}^o{}_2]^{4+}$ with relative energies (from DFT calculations, chains omitted, see the Supporting Information, section 4); b) crystal structure of *cis*-$[Pd(\textit{up}\text{-2-pic})_2(\textit{down}\text{-2-pic})_2](BF_4)_2$ with counter-ions omitted for clarity; c) experimental and theoretical PXRD patterns.

Heteroleptic assembly from two different ligand backbones

Having successfully validated this strategy for the acridone-based heteroleptic cage *cis*-$[Pd_2\mathbf{A}^i{}_2\mathbf{A'}^o{}_2]^{4+}$, we moved on to examine whether the picoline 'in$_2$/out$_2$' approach can foster the assembly of heteroleptic Pd^{II} cages from two chemically distinct backbones.

Since the Pd-mediated self-assembly of phenothiazine-derived banana-shaped ligands is well described,[9a] we chose to investigate the self-sorting of picolyl ligands $\mathbf{P}^i$ and $\mathbf{P}^o$ with the already established ligands $\mathbf{A}^i$ and $\mathbf{A}^o$. Homoleptic assemblies from $\mathbf{P}^i$ and $\mathbf{P}^o$ were found to be of analogous composition to that observed for the acridone ligands. Reacting $\mathbf{P}^i$ with $[Pd(CH_3CN)_4](BF_4)_2$ in a 2:1 ratio at room temperature gave a single homoleptic species, identified as bowl-shaped $[Pd_2\mathbf{P}^i{}_3(CD_3CN)_2]^{4+}$ by NMR spectroscopy and ESI mass spectrometry (Figure S46 and S47). Under similar conditions, reacting $\mathbf{P}^o$ and $[Pd(CH_3CN)_4](BF_4)_2$ gave a 4:1 mixture of the $[Pd_2\mathbf{P}^o{}_3(CD_3CN)_2]^{4+}$ bowl and $[Pd_2\mathbf{P}^o{}_2(CD_3CN)_4]^{4+}$ ring. The homoleptic phenothiazine structures were further confirmed by ESI-MS and 2D NMR analysis (Figure S36–S39).

Heating a 1:1:1 mixture of $\mathbf{A'}^o$, $\mathbf{P}^i$ and $[Pd(CH_3CN)_4](BF_4)_2$ for 8 h to 70 °C resulted in a relatively simple ^{1}H NMR spectrum with 12 distinct aromatic signals (Figure 5a–c). Further analysis of the sample by ESI-MS revealed prominent signals at $m/z=$ 578.7, 800.6 and 1244.4, which correspond to the formula $[Pd_2\mathbf{A'}^o{}_2\mathbf{P}^i{}_2+n\,BF_4]^{(4-n)+}$ ($n=0$–2) (Figure 5d). Again, NOESY analysis showed the characteristic cross peaks between $H_f\cdots H_{g'}$ and $H_{f'}\cdots H_g$, indicative of the adjacent positioning of ligands in a *cis*-$[Pd_2\mathbf{A'}^o{}_2\mathbf{P}^i{}_2]^{4+}$ assembly (Figure S51). Additionally, a DOSY experiment confirmed that all assigned proton signals of $[Pd_2\mathbf{A'}^o{}_2\mathbf{P}^i{}_2]^{4+}$ belong to the same diffusion coefficient (Figure S52).

On the other hand, a 1:1:1 mixture of $\mathbf{A}^i$, $\mathbf{P}^o$ and $[Pd(CH_3CN)_4](BF_4)_2$ produced a rather convoluted ^{1}H NMR spec-

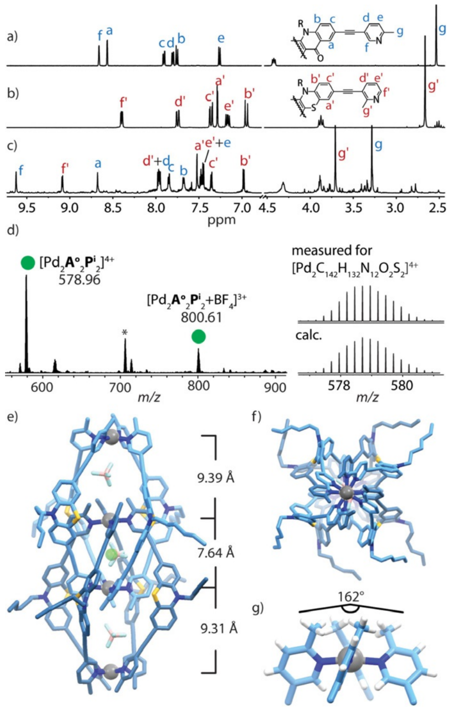

Figure 5. ^{1}H NMR spectra (500 MHz/CD_3CN) of a) **A′^{o}**; b) **P^i**; c) $[Pd_2\mathbf{A'^o}_2\mathbf{P^i}_2]^{4+}$ obtained by heating a 1:1:1 mixture of **A′^{o}**, **P^i** and Pd^{II} to 70 °C; d) ESI-MS spectrum of $[Pd_2\mathbf{A'^o}_2\mathbf{P^i}_2+n\,BF_4]^{(4-n)+}$ with $n=0$, 1 ($*=[Pd_2\mathbf{A'^o}_3\mathbf{P^i}_2]^{4+}$). X-ray structure of $[(BF_4)_{2.4}Cl_{0.6}@Pd_4\mathbf{P^o}_8]^{5+}$ with both found anions shown superimposed in the central cavity. Hydrogen atoms and unbound counter-ions were removed for clarity; e) side view, showing the Pd⋯Pd distances, f) top view; g) a close-up view of the outer picoline$_4$-Pd fragment of the structure.

trum, with multiple overlapping sets of proton signals (Figure S53). Two sets of signals were assigned to the $[Pd_2\mathbf{A^i}_3(CD_3CN)_2]^{4+}$ bowl-shaped assembly (Figure S54), but assemblies of **P^o** could not be clearly identified. However, when a similar mixture was microwave-irradiated followed by heating to 70 °C overnight, the ESI MS spectra revealed the prominent formation of heteroleptic $[Pd_2\mathbf{A^i}_2\mathbf{P^o}_2]^{4+}$ cage (Figure S58). While we cannot provide definite reasons for the different behavior of this ligand combination, the results show that the backbone structures (flat acridone vs. bent phenothiazine) seem to influence the steric preferences around the metal centers.

We were successful, in this case, in obtaining single crystals by slow evaporation of the CD_3CN reaction mixture. Single-crystal X-ray analysis, however, revealed a rather unexpected structure: an interpenetrated double-cage with the formula $[(BF_4)_{2.4}Cl_{0.6}@Pd_4\mathbf{P^o}_8]^{5+}$ (Figure 5 e,f). In accordance with previous examples,[7,9b,10a,25] the partitioned cavity of this dimeric cage features three pockets, with two outer pockets occupied by BF_4^- anions. The central cavity, however, is partially occupied by BF_4^- and Cl^- (ratio: 40:60 %). We note that strong chloride binding in the double-cages is known, even by trapping chloride that is present in trace impurities.[25] The Pd⋯Pd distance of this cavity is therefore shorter than the one of the outer pockets (7.64 Å vs. 9.39 Å), although the picolines' methyl groups occupy a portion of the two outer cavities. In order to relieve the steric crowding caused by the all-*syn* arrangement of the methyl substituents around the Pd^{II} centers, the picoline donors are tilted by up to 18° (Figure 5 g) with respect to the ideal square planar arrangement, though the apparent strain seems to be counteracted by close contacts between the methyl substituents and BF_4^- anions. Each phenothiazine backbone undergoes π-stacking with the picoline donor from an adjacent ligand (belonging to the catenated cage unit), providing additional stabilization in the double-cage structure. In addition, the slightly folded structure of **P^o** (with respect to the aromatic face of the tricyclic backbone) may help in arranging all of the methyl groups on one side of the Pd^{II} planes by allowing the picoline donors to adopt a pronouncedly tilted propeller arrangement around the metal centers. In contrast, the flat acridone backbone would favor a more perpendicular orientation of the donor ring planes with respect to the Pd^{II} plane, a situation that would be sterically demanding.[10a]

This observation impressively showed up the possibility of forming homoleptic cages with all four methyl groups on the same face of the Pd(picoline)$_4$ complex, when a suitable avenue is opened to a self-assembly product of exceptional thermodynamic stability. As we observed in previous work,[7b,25c] the anion-templated formation of interpenetrated double-cages can lead into such an energetic sink, here causing the system to override the pivotal steric control, in other cases leading towards heteroleptic cages.

In order to gain more insight into this situation, we tried to reproduce the formation of this double-cage by heating a mixture of **P^o**, $[Pd(CH_3CN)_4](BF_4)_2$ and Cl^- ions in a ratio of 8:4:1 at 70 °C for several hours. While this procedure did not lead to conclusive results, we opted for even harsher conditions and subjected the reaction mixture to microwave irradiation followed by heating to 70 °C overnight. Then, indeed, clear NMR spectroscopic and mass spectrometric evidence for the formation of interpenetrating double-cage $[(BF_4)_2Cl@Pd_4\mathbf{P^o}_8]^{5+}$ could be collected, along with signatures for the formation of bowl $[Pd_2\mathbf{P^o}_3]^{4+}$ as minor product (double-cage:bowl ≈1:0.6; Figure 6). Further evidence for the double-cage was provided by ^{1}H -^{1}H NOESY analysis, which exhibited important cross peaks between the **P^o** ligands of the interpenetrated subunits such as H_f⋯$H_{g''}$ and $H_{g'}$⋯H_a (Figure S41). The ESI MS spectrum of the sample (Figure 6 c and S42) revealed a prominent peak corresponding to $[(BF_4)_2Cl@Pd_4\mathbf{P^o}_8]^{5+}$ double-cage. The observations were thus in full agreement with the structure elucidated through single crystal XRD analysis.

Conclusions

A new strategy to access discrete *cis*-$[Pd_2\mathbf{L}_2\mathbf{L'}_2]^{4+}$ coordination cages has been developed through the exploitation of the steric crowding of picoline donors around square-planar coordinated Pd^{II} cations. Studies of homoleptic cage formation clearly demonstrated that $[Pd_2\mathbf{L}_4]$ cages are not easily accessed when the picoline methyl substituents point in the same direction (either inside or outside the cavity). In such cases, $[Pd_2\mathbf{L}_3(solvent)_2]^{4+}$ bowl and $[Pd_2\mathbf{L}_2(solvent)_4]^{4+}$ ring species were isolated under kinetic control. On the other hand, combining the ligands suitable for an 'in$_2$/out$_2$' orientation of pico-

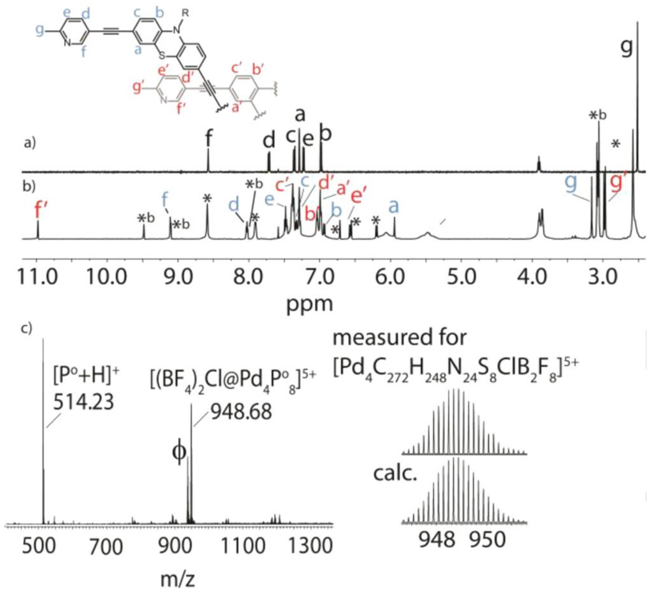

Figure 6. ^1H NMR spectra (500 MHz/CD_3CN) of a) **P°**; b) [$(BF_4)_2Cl@Pd_4$**P°**$_8$]$^{5+}$ obtained by microwave irradiation, followed by heating, of a 8:4:1 mixture of **P°**, [$Pd(CH_3CN)_4$]$(BF_4)_2$ and Cl^- (*b and * = [Pd_2**P°**$_3$] bowl and other side products); c) ESI-MS spectrum of [$(BF_4)_2Cl@Pd_4$**P°**$_8$]$^{5+}$ (ϕ = [$BF_4Cl_2@Pd_4$**P°**$_8$]$^{5+}$).

line donors in a 1:1 ratio resulted in the clean formation of *cis*-[Pd_2**L**$_2$**L′**$_2$] cages under thermodynamic control. We were able to show this both for cages composed of four acridone backbones and for cages composed of pairs of acridone and phenothiazine backbones, thus validating the scope of this approach.

In the latter example, the different outcomes of self-assembly point towards the fine geometric balance that drives the formation of heteroleptic [Pd_2**L**$_2$**L′**$_2$] cages over double-cages; the latter being thermodynamically favored in certain circumstances. In particular, the observed differences in the self-sorting outcomes between the two possible combinations of the acridone and phenothiazine regioisomeric ligands (**A°**/ **P**^{i} and **A**^{i}/ **P°**) may in part be related to their propensity to form double-cage structures. Although the crystal structure of [$(BF_4)_{2.4}Cl_{0.6}@Pd_4$**P°**$_8$]$^{5+}$ may be considered an isolated example, it does point to the fact that the double-cage structure is kinetically and thermodynamically very stable. With this in mind, the successful formation of the heteroleptic [Pd_2**A°**$_2$**P**$^{i}_2$]$^{4+}$ structure most likely relates to the inability of both of these ligands to form double-cages: the picoline donors of **P**^{i} hinder cage-catenation due to steric crowing of the methyl groups, eight of which would all have to reside inside the tentative double-cage's inner pocket. For **A°**, the flat acridone backbone may not afford the tilted geometry for this sterically demanding picolyl-based dimeric-cage structure.

Interestingly, the folded nature of the phenothiazine backbones also affects heteroleptic cage formation when they are present in both ligands (i.e. in the system **P**^{i} plus **P°**). Here, a mixture of species was found to be formed, containing different heteroleptic species as well as homoleptic side products (including the observed double-cage). In contrast, inside/outside ligand mixtures based on flat acridone alone, as well as the combination of acridone **A′°** and bent phenothiazine **P**^{i} afforded clean [Pd_2**L**$_2$**L′**$_2$] cages.

Further investigations using the herein introduced [Pd_2**L**$_2$**L′**$_2$] cage motif to study the interplay between rationally combined functionalities such as donor-acceptor systems, tailored receptors and multifunctional catalysts are currently underway in our laboratory.

Acknowledgements

We thank Dr. M. John (Georg-August University Göttingen) and Prof. Dr. W. Hiller (TU Dortmund) for assistance with NMR measurements and helpful discussions. We thank Dr. Andreas Brockmeyer and Dr. Petra Janning (Max-Planck Institute for Molecular Physiology, Dortmund) and Dr. Holm Frauendorf (Georg-August University Göttingen) for mass spectra measurements. Diffraction data for [$(BF_4)_{2.4}Cl_{0.6}@Pd_4$**P°**$_8$]$^{5+}$ was collected at PETRA III at DESY,[26] a member of the Helmholtz Association (HGF). The authors thank Dr. Anja Burkhardt for assistance in using synchrotron beamline P11 (I-20160736). R.Z. thanks the China Scholarship Council for a PhD fellowship. W.M.B thanks the Alexander von Humboldt Foundation for a postdoctoral fellowship. We thank the Fonds der Chemischen Industrie, the Deutsche Forschungsgemeinschaft (CL 489/2-2 and GRK 2376) and the European Research Council (ERC Consolidator grant 683083, RAMSES = Reactivity and Assembly of Multifunctional, Stimuli-responsive Encapsulation Structures) for their support.

Conflict of interest

The authors declare no conflict of interest.

Keywords: coordination cages · heteroleptic assembly · self-sorting · steric control · supramolecular chemistry

[1] a) S. De, K. Mahata, M. Schmittel, *Chem. Soc. Rev.* **2010**, *39*, 1555 – 1575; b) M. L. Saha, M. Schmittel, *Org. Biomol. Chem.* **2012**, *10*, 4651 – 4684; c) H. Li, Z.-J. Yao, D. Liu, G.-X. Jin, *Coord. Chem. Rev.* **2015**, *293 – 294*, 139 – 157; d) M. M. Safont-Sempere, G. Fernández, F. Würthner, *Chem. Rev.* **2011**, *111*, 5784 – 5814; e) M. M. J. Smulders, I. A. Riddell, C. Browne, J. R. Nitschke, *Chem. Soc. Rev.* **2013**, *42*, 1728 – 1754; f) S. Mukherjee, P. S. Mukherjee, *Chem. Commun.* **2014**, *50*, 2239 – 2248.
[2] a) P. Baxter, J.-M. Lehn, A. DeCian, J. Fischer, *Angew. Chem. Int. Ed. Engl.* **1993**, *32*, 69 – 72; *Angew. Chem.* **1993**, *105*, 92 – 95; b) P. N. W. Baxter, J.-M. Lehn, G. Baum, D. Fenske, *Chem. Eur. J.* **1999**, *5*, 102 – 112.
[3] M. Schmittel, A. Ganz, *Chem. Commun.* **1997**, 999 – 1000.
[4] a) M. L. Saha, S. De, S. Pramanik, M. Schmittel, *Chem. Soc. Rev.* **2013**, *42*, 6860 – 6909; b) M. L. Saha, S. Neogi, M. Schmittel, *Dalton Trans.* **2014**, *43*, 3815 – 3834; c) N. Mittal, M. L. Saha, M. Schmittel, *Chem. Commun.* **2016**, *52*, 8749 – 8752.
[5] M. Yoshizawa, M. Nagao, K. Kumazawa, M. Fujita, *J. Organomet. Chem.* **2005**, *690*, 5383 – 5388.
[6] a) Q.-F. Sun, S. Sato, M. Fujita, *Angew. Chem. Int. Ed.* **2014**, *53*, 13510 – 13513; *Angew. Chem.* **2014**, *126*, 13728 – 13731; b) P. Howlader, P. Das, E. Zangrando, P. S. Mukherjee, *J. Am. Chem. Soc.* **2016**, *138*, 1668 – 1676; c) T. R. Cook, P. J. Stang, *Chem. Rev.* **2015**, *115*, 7001 – 7045; d) W. M. Bloch, G. H. Clever, *Chem. Commun.* **2017**, *53*, 8506 – 8516.
[7] a) M. Han, D. M. Engelhard, G. H. Clever, *Chem. Soc. Rev.* **2014**, *43*, 1848 – 1860; b) M. Frank, M. D. Johnstone, G. H. Clever, *Chem. Eur. J.* **2016**, *22*, 14104 – 14125.

[8] a) M. Han, R. Michel, B. He, Y.-S. Chen, D. Stalke, M. John, G. H. Clever, *Angew. Chem. Int. Ed.* **2013**, *52*, 1319–1323; *Angew. Chem.* **2013**, *125*, 1358–1362; b) A. Díaz-Moscoso, P. Ballester, *Chem. Commun.* **2017**, *53*, 4635–4652.
[9] a) M. Frank, J. Hey, I. Balcioglu, Y.-S. Chen, D. Stalke, T. Suenobu, S. Fukuzumi, H. Frauendorf, G. H. Clever, *Angew. Chem. Int. Ed.* **2013**, *52*, 10102–10106; *Angew. Chem.* **2013**, *125*, 10288–10293; b) M. Frank, J. Ahrens, I. Bejenke, M. Krick, D. Schwarzer, G. H. Clever, *J. Am. Chem. Soc.* **2016**, *138*, 8279–8287; c) J. Ahrens, M. Frank, G. H. Clever, D. Schwarzer, *Phys. Chem. Chem. Phys.* **2017**, *19*, 13596–13603; d) K. Yazaki, S. Noda, Y. Tanaka, Y. Sei, M. Akita, M. Yoshizawa, *Angew. Chem. Int. Ed.* **2016**, *55*, 15031–15034; *Angew. Chem.* **2016**, *128*, 15255–15258; e) S. Bivaud, J.-Y. Balandier, M. Chas, M. Allain, S. Goeb, M. Sallé, *J. Am. Chem. Soc.* **2012**, *134*, 11968–11970; f) K. Mahata, P. D. Frischmann, F. Würthner, *J. Am. Chem. Soc.* **2013**, *135*, 15656–15661.
[10] a) S. Löffler, J. Lübben, L. Krause, D. Stalke, B. Dittrich, G. H. Clever, *J. Am. Chem. Soc.* **2015**, *137*, 1060–1063; b) N. Kishi, Z. Li, K. Yoza, M. Akita, M. Yoshizawa, *J. Am. Chem. Soc.* **2011**, *133*, 11438–11441; c) N. Kishi, Z. Li, Y. Sei, M. Akita, K. Yoza, J. S. Siegel, M. Yoshizawa, *Chem. Eur. J.* **2013**, *19*, 6313–6320; d) D. P. August, G. S. Nichol, P. J. Lusby, *Angew. Chem. Int. Ed.* **2016**, *55*, 15022–15026; *Angew. Chem.* **2016**, *128*, 15246–15250.
[11] a) S. Löffler, J. Lübben, A. Wuttke, R. A. Mata, M. John, B. Dittrich, G. H. Clever, *Chem. Sci.* **2016**, *7*, 4676–4684; b) M. D. Johnstone, E. K. Schwarze, J. Ahrens, D. Schwarzer, J. J. Holstein, B. Dittrich, F. M. Pfeffer, G. H. Clever, *Chem. Eur. J.* **2016**, *22*, 10791–10795; c) L.-P. Zhou, Q.-F. Sun, *Chem. Commun.* **2015**, *51*, 16767–16770.
[12] a) J. E. M. Lewis, E. L. Gavey, S. A. Cameron, J. D. Crowley, *Chem. Sci.* **2012**, *3*, 778–784; b) S. M. McNeill, D. Preston, J. E. M. Lewis, A. Robert, K. Knerr-Rupp, D. O. Graham, J. R. Wright, G. I. Giles, J. D. Crowley, *Dalton Trans.* **2015**, *44*, 11129–11136.
[13] M. Krick, J. Holstein, C. Würtele, G. H. Clever, *Chem. Commun.* **2016**, *52*, 10411–10414.
[14] a) M. Han, J. Hey, W. Kawamura, D. Stalke, M. Shionoya, G. H. Clever, *Inorg. Chem.* **2012**, *51*, 9574–9576; b) R. Zhu, J. Lübben, B. Dittrich, G. H. Clever, *Angew. Chem. Int. Ed.* **2015**, *54*, 2796–2800; *Angew. Chem.* **2015**, *127*, 2838–2842.
[15] a) M. Frank, L. Krause, R. Herbst-Irmer, D. Stalke, G. H. Clever, *Dalton Trans.* **2014**, *43*, 4587–4592; b) A. M. Johnson, R. J. Hooley, *Inorg. Chem.* **2011**, *50*, 4671–4673.
[16] a) M. Yamashina, T. Yuki, Y. Sei, M. Akita, M. Yoshizawa, *Chem. Eur. J.* **2015**, *21*, 4200–4204; b) D. Preston, J. E. Barnsley, K. C. Gordon, J. D. Crowley, *J. Am. Chem. Soc.* **2016**, *138*, 10578–10585.
[17] W. M. Bloch, Y. Abe, J. J. Holstein, C. M. Wandtke, B. Dittrich, G. H. Clever, *J. Am. Chem. Soc.* **2016**, *138*, 13750–13755.
[18] W. M. Bloch, J. J. Holstein, W. Hiller, G. H. Clever, *Angew. Chem. Int. Ed.* **2017**, *56*, 8285–8289; *Angew. Chem.* **2017**, *129*, 8399–8404.
[19] In solution, CD_3CN or H_2O molecules may as well occupy these labile coordination sites.
[20] Shivakumaraiah, N. M. N. Gowda, *J. Chem. Res.* **2005**, *2005*, 505–507.
[21] K. Yazaki, Y. Sei, M. Akita, M. Yoshizawa, *Chem. Eur. J.* **2016**, *22*, 17557–17561.
[22] a) S.-Y. Chang, H.-Y. Jang, K.-S. Jeong, *Chem. Eur. J.* **2004**, *10*, 4358–4366; b) T. Rama, C. Alvariño, O. Domarco, C. Platas-Iglesias, V. Blanco, M. D. García, C. Peinador, J. M. Quintela, *Inorg. Chem.* **2016**, *55*, 2290–2298.
[23] a) Q. Zhang, L. He, J.-M. Liu, W. Wang, J. Zhang, C.-Y. Su, *Dalton Trans.* **2010**, *39*, 11171–11179; b) F. A. Pereira, T. Fallows, M. Frank, A. Chen, G. H. Clever, *Z. Anorg. Allg. Chem.* **2013**, *639*, 1598–1605.
[24] M. Palaniandavar, I. Somasundaram, M. Lakshminarayanan, H. Manohar, *J. Chem. Soc. Dalton Trans.* **1996**, 1333–1340.
[25] a) M. Frank, J. M. Dieterich, S. Freye, R. A. Mata, G. H. Clever, *Dalton Trans.* **2013**, *42*, 15906–15910; b) S. Freye, J. Hey, A. Torras-Galán, D. Stalke, R. Herbst-Irmer, M. John, G. H. Clever, *Angew. Chem. Int. Ed.* **2012**, *51*, 2191–2194; *Angew. Chem.* **2012**, *124*, 2233–2237; c) S. Freye, R. Michel, D. Stalke, M. Pawliczek, H. Frauendorf, G. H. Clever, *J. Am. Chem. Soc.* **2013**, *135*, 8476–8479.
[26] A. Burkhardt, T. Pakendorf, B. Reime, J. Meyer, P. Fischer, N. Stübe, S. Panneerselvam, O. Lorbeer, K. Stachnik, M. Warmer, P. Roedig, D. Goeries, A. Meents, *Eur. Phys. J. Plus* **2016**, *131*, 56.

Manuscript received: May 2, 2018
Accepted manuscript online: June 20, 2018
Version of record online: July 30, 2018

